

Macroporous Hydrogel for High-Performance Atmospheric Water Harvesting

Tong Lyu, Zhaoyang Wang, Ruonan Liu, Kun Chen, He Liu, and Ye Tian*

Cite This: *ACS Appl. Mater. Interfaces* 2022, 14, 32433–32443

Read Online

ACCESS |



Metrics & More



Article Recommendations



Supporting Information

ABSTRACT: Simple, low-cost, and high-performance atmospheric water harvesting (AWH) still remains challenging in the context of global water shortage. Here, we present a simple and low-cost macroporous hydrogel for high-performance AWH to address this challenge. We employed an innovative strategy of pore foaming and vacuum drying to rationally fabricate a macroporous hydrogel. The hydrogel is endowed with a macroporous structure and a high specific surface area, enabling sufficient contact of the inner sorbent with outside air and high-performance AWH. The experiments demonstrate that macroporous hydrogels can achieve high-performance AWH with a broad range of sorption humidity [relative humidity (RH) from 100% to even lower than 20%], high water sorption capacity (highest 433.72% of hydrogel's own weight at ~98% RH, 25 °C within 60 h), rapid vapor capturing (the sorption efficiency is as high as 0.32 g g⁻¹ h⁻¹ in the first 3 h at 90% RH, 25 °C), unique durability, low desorption temperature (~50 °C, lowest), and high water-releasing rate (release 99.38% of the sorbed water under 500 W m⁻² light for 6 h). The results show that this macroporous hydrogel can sorb water more than 193.46% of its own weight overnight (13 h) at a RH of ~90%, 25 °C and release as high as 99.38% of the sorbed water via the photothermal effect. It is estimated that the daily water yield can reach up to approximately 2.56 kg kg⁻¹ day⁻¹ in real outdoor conditions, enabling daily minimum water consumption of an adult. Our simple, affordable, and easy-to-scale-up macroporous hydrogel can not only unleash the unlimited possibilities for large-scale and high-performance AWH but also offer promising opportunities for functional materials, soft matter, flexible electronics, tissue engineering, and biomedical applications.

KEYWORDS: hydrogel, water collection, atmospheric water harvesting, macroporous hydrogel, polymer



INTRODUCTION

Water shortage has become one of the most serious problems in the world. What is worse, the number of people suffering from water scarcity keeps increasing.¹ It is critical to find a solution to alleviate or end this crisis. Atmospheric water harvesting (AWH) has been brought up as a corresponding solution to water issues. AWH is the technique that captures water from ambient air in either the liquid form or gas state and is then released in the form of liquid water. It is reported that 12,900 billion tons of fresh water is preserved in the atmosphere;² therefore, AWH is a promising approach to produce fresh water and alleviate the water crisis.

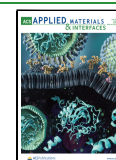
There are several AWH strategies that have been developed over the years. Some dewing-based large AWH systems can collect atmospheric water effectively.^{3–5} However, these costly AWH systems consume too much energy and need extra attention to maintain the systems. Thus, it is severely limited to facilities in remote and/or poor areas with water shortages.⁶ Another AWH strategy is fog collection using surface morphology through biomimetic structures,^{7,8} for instance, spider-silk,^{9,10} cactus,^{11,12} desert beetle,^{13,14} and other natural

living beings,^{15–18} to transport and gather water droplets. However, the manufacturing procedures of the biomimetic surfaces are strenuous, complex, and time-consuming. In addition, the sophisticated structures and well-designed surfaces not only are prone to damage but also require high humidity, yet they exhibit low water collection efficiency. The sorption-based AWH method on MOF derivatives,¹⁹ inorganic materials,^{20–23} and polymeric hydrogels is also a good strategy for harvesting water from the atmosphere. MOF-based AWH has considerable water yield even at very low relative humidity (RH).^{24,25} Unfortunately, its high cost and complicated preparation process cause the inconvenience of deployment in distressed areas,⁶ resulting in the limitation of its large-scale applications. Inorganic materials, like silica gel,²⁶ sawdust,²⁰ and sand,²⁷

Received: March 9, 2022

Accepted: June 28, 2022

Published: July 8, 2022



Scheme 1. Fabrication of LCP Hydrogel^a

^aSchematic illustration of the fabrication process of LCP hydrogel.

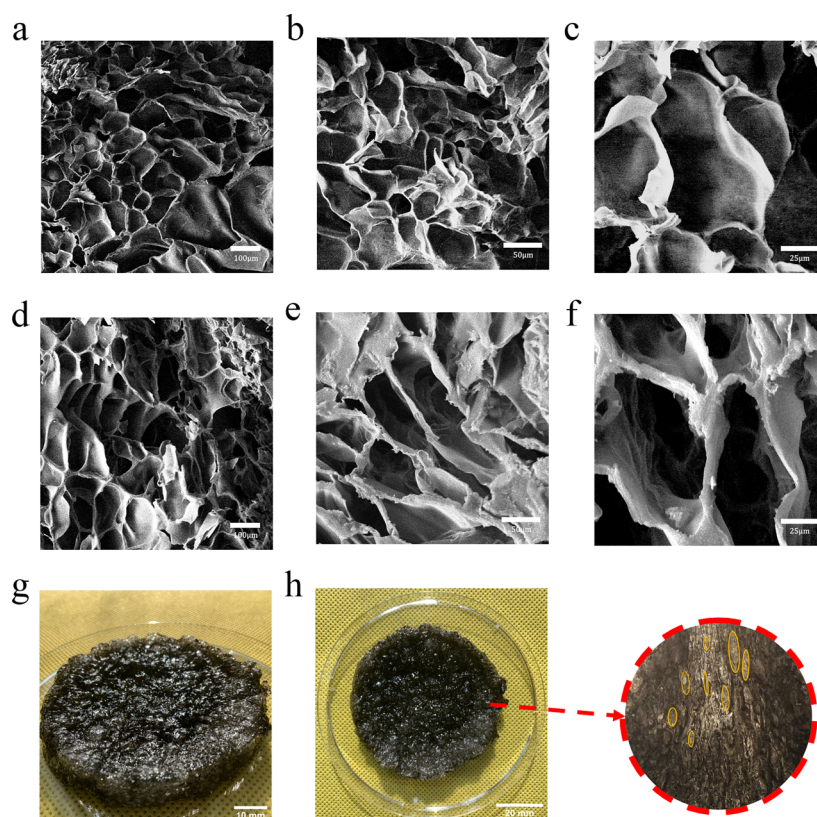


Figure 1. Characterization of LCP hydrogel. SEM images of (a–c) dehydrated CNT-PAM hydrogel and (d–f) PEG-400-doped CNT-PAM hydrogel in different magnifications. (g,h) Photographs of the same LCP hydrogel and the partial enlarged detail show the distinct macrostructure throughout the hydrogel.

embedded with hygroscopic salts, have served well in AWH. However, they may suffer from poor control over the macrostructures of the materials (e.g., the interspaces of sawdust and labile form of sands), so that the performance of water harvesting is heavily affected. On the contrary, polymeric hydrogels can be easily adjusted and precisely tailored for AWH. However, the traditional hydrogel-based AWH strategy generally has the issue of slow water sorption. This is because the water sorption of the hydrogel happens progressively from the outside surface to the core of the blocky hydrogel. Later, the

salt particles on the surface agglomerate and form passivation layers, and the water vapor permeability is considerably decreased, resulting in the extension of sorption time.^{28,29} Therefore, there is an urgent demand to develop a simple and economical AWH technique for large-scale and high-performance water collection from the atmosphere.

Herein, we introduce a simple and low-cost macroporous hydrogel for high-performance AWH with rapid water sorption and high water desorption rates, composed of lithium chloride, polyacrylamide (PAM), and a light dose of carbon nanotubes

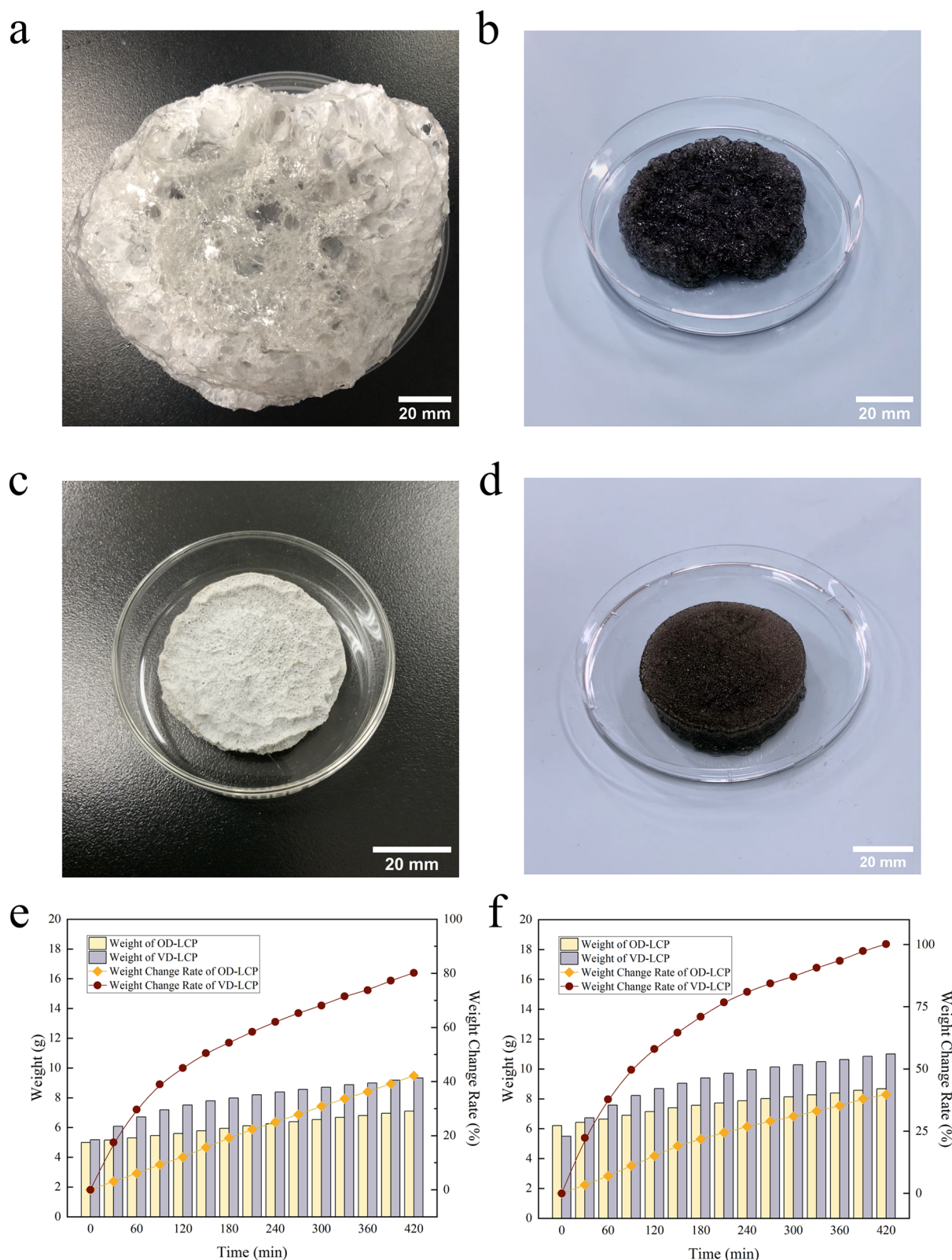


Figure 2. Sorption discrepancy between VD-LCP and OD-LCP hydrogel. Photographs of (a) dehydrated VD-LCP hydrogel, (b) hydrated VD-LCP hydrogel, (c) dehydrated OD-LCP hydrogel, and (d) hydrated OD-LCP hydrogel. Weight and weight change rate of VD-LCP hydrogel and OD-LCP hydrogel at (e) 60–70% and (f) 70–80% RH.

(named LCP hydrogel). We use an unorthodox and simple pore-foaming and vacuum-drying (PFVD) method to prepare a low-cost macroporous hydrogel (~2.83 USD per kg, Table S1). The macroporous structure provides a high specific surface area,

ensuring the effective and large-scale contact between humid air and the inner sorbents. Compared with other sorption-based AWH using hydrogel substrates, LCP hydrogels can swiftly let water infiltrate the whole hydrogel bulk without obvious

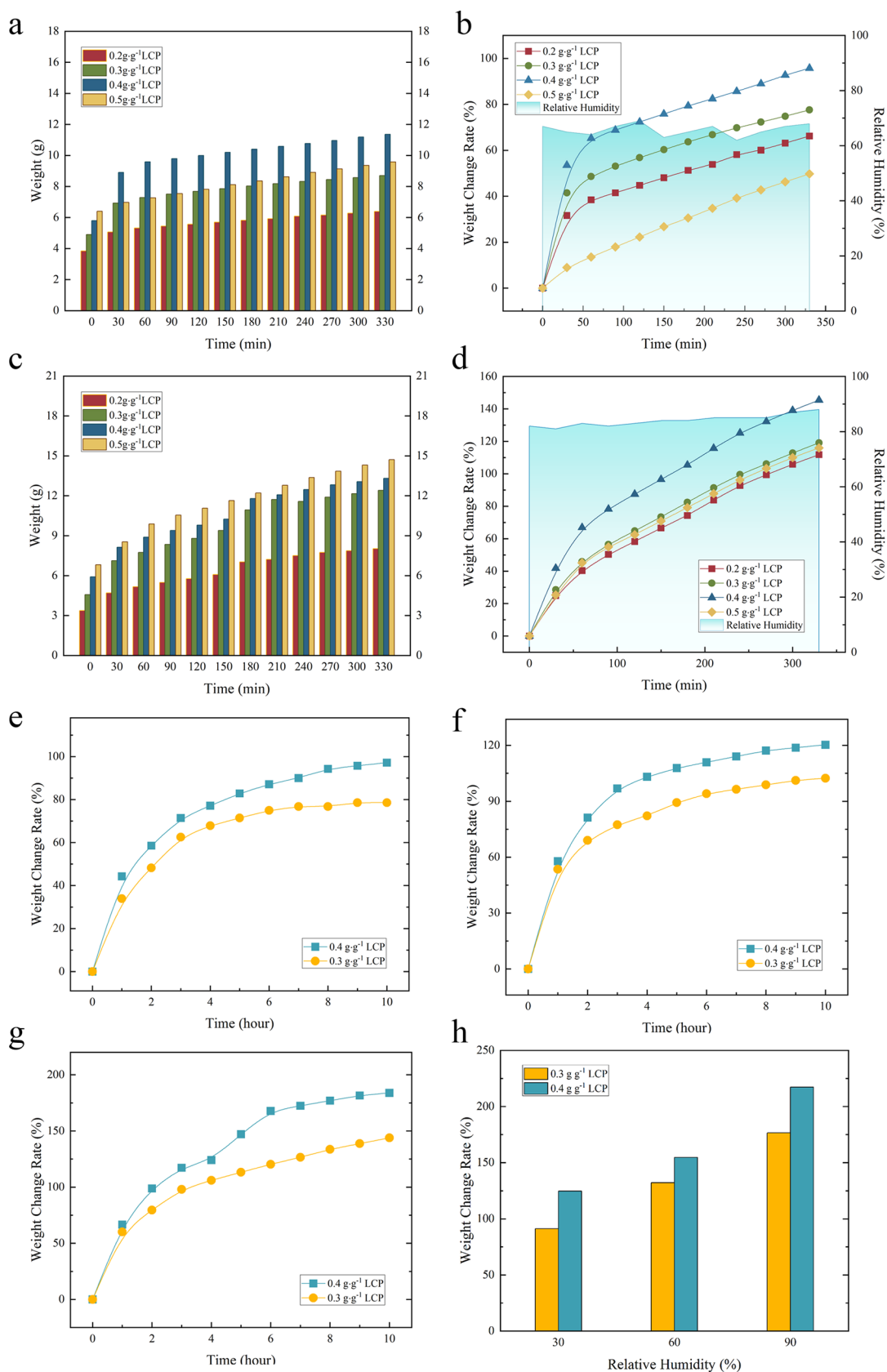


Figure 3. Water sorption ability. (a) Weight of LCP hydrogels with the LiCl concentrations of 0.2, 0.3, 0.4, and 0.5 g g⁻¹ at 60–70% RH. (b) Weight change rate of LCP hydrogel with the LiCl concentrations of 0.2, 0.3, 0.4, and 0.5 g g⁻¹ at 60–70% RH. (c) Weight of LCP hydrogels with the LiCl concentrations of 0.2, 0.3, 0.4, and 0.5 g g⁻¹ at 80–90% RH. (d) Weight change rate of LCP hydrogel with the LiCl concentrations of 0.2, 0.3, 0.4, and 0.5 g g⁻¹ at 80–90% RH. Weight change rate of LCP hydrogels with LiCl concentrations of 0.3 and 0.4 g g⁻¹ at (e) 30% RH, (f) 60% RH, and (g) 90% RH within 10 h. (h) Weight change rates of LCP hydrogels with LiCl concentrations of 0.3 and 0.4 g g⁻¹ at 30, 60, and 90% RH in 24 h, respectively.

passivation layers. The LCP hydrogels can harvest atmospheric water with a broad range of sorption humidity (RH from 100% to even lower than 20%), high water sorption capacity (highest with $\sim 433.72\%$ of hydrogel's own weight), rapid vapor capturing ($0.32 \text{ g g}^{-1} \text{ h}^{-1}$ in the first 3 h at 90% RH, 25 °C), unique durability, low desorption temperature (~ 50 °C, lowest), and high water desorption rate (release 99.38% of the sorbed water), showing high-performance AWH. In addition, LCP hydrogels can sorb 1.93 g g^{-1} water overnight (13 h) at RH 90% and easily release up to 99.38% of the sorbed water via the photothermal effect under 500 W m^{-2} light. It is estimated that the daily water yield can reach up to approximately $2.56 \text{ kg kg}^{-1} \text{ day}^{-1}$ with three cycles, enabling more than the average of water drunk by an adult daily.^{30,31} Our macroporous hydrogel is a promising candidate for large-scale and high-performance AWH, functional materials, soft matter, flexible electronics, and biomedical applications.

RESULTS AND DISCUSSION

Synthesis and Characterization of the LCP Hydrogel.

We employed an innovative strategy of PFVD to rationally and cheaply (2.83 USD per kg) fabricate a macroporous LCP hydrogel (Scheme 1). The macroporous structure of the LCP hydrogel was mainly attributable to a joint effort of pore-foaming agent PEG-400 and vacuum-drying process. Initially, PEG-400 was embedded into the hydrogel network and caused the change of the whole hydrogel network. After the removal of PEG-400, the initial porous structure of the hydrogel was formed. Then, the hydrogel was freeze-dried and loaded with lithium chloride (LiCl). LiCl-loaded hydrogel obtained good mechanical strength, flexibility, and swelling properties. During the second freeze-drying, the initial porous structure was greatly stretched and magnified under a vacuum condition so that the shaggy and macroporous hydrogel was synthesized. Compared with the scanning electron microscopy (SEM) images of the PAm hydrogel without PEG (Figure 1a–c), the PEG-400-doped PAm hydrogel presented the thicker walls of hydrogel networks, bigger pore diameter, and more three-dimensional pore structure (Figure 1d–f). Actually, PEG with different molecular weights has a significant effect on the mechanical strength and swelling property of the hydrogel as AWH's substrate. Macromolecular PEG greatly enlarges the pore size of the hydrogel and enhances the swelling property of hydrogel. Unfortunately, the macromolecular PEG can also reduce the mechanical property of the hydrogel,³² and the re-swelling capacity of the hydrogel is reduced due to the collapsed pore walls and the blocked pore channels. However, PEG, with low molecular weights, like PEG-400, can improve and maintain hydrogel's swelling properties, even when re-swelling. Hence, we use easy-removed PEG-400 to create uniform macropores within hydrogels for increasing the water capacity of the hydrogel substrate. FTIR image shows that PEG-400 was mostly removed from the hydrogel after soaking in DI water for 24 h (Figure S1). The resultant LCP hydrogel doped by PEG-400 has orderly and obviously arranged macropores, even after water sorption (Figure 1g,h), enabling high-performance AWH.

It is worth mentioning that the last freeze-drying procedure instead of oven-drying also plays an important role in the macroporous structure of LCP hydrogel. Compared with traditional oven-drying, we use the freeze-drying technique to surprisingly realize better hydrophilicity of vacuum-dried (VD) CNT-PAm hydrogel than that of oven-dried (OD) CNT-PAm hydrogel (Movie S1) and bigger pores of LCP hydrogel. After

soaking the CNT-PAm hydrogel into LiCl aqueous solution, the LCP hydrogel with certain LiCl concentration could not be frozen in a freeze-dry machine and maintain good mechanical strength, flexibility, and swelling properties due to the immersion wetting of LiCl. The gas encapsulated into the LCP hydrogel was immediately expanded under the vacuum conditions so that the pores of the LCP hydrogel were stretched and enlarged obviously. Finally, the gas was expelled from the LCP hydrogel due to the increasing vacuum degree, then the shaggy and macroporous structure of the LCP hydrogel was left. As presented in Figure 2a–d, the VD-LCP hydrogel has much bigger pores and volume than the OD-LCP hydrogel in both dehydrated and hydrated states. Therefore, the VD-LCP hydrogel has a high specific surface area, resulting in sufficient contact of inner sorbents and outside air and high-performance AWH. In addition, water sorption tests of VD-LCP hydrogel and OD-LCP hydrogel show that the VD-LCP hydrogel certainly has a better performance than the OD-LCP hydrogel (Figure 2e,f). The weights of OD-LCP hydrogel and VD-LCP hydrogel increased from 4.998 and 5.176 g to 7.106 and 9.327 g, indicating that they sorbed 42.18 and 80.20% of their original weights at 60–70% RH, ~ 20 °C, respectively. The sorption test at 70–80% RH and a temperature of ~ 20 °C showed that a 6.209 g OD-LCP hydrogel and a 5.497 g VD-LCP hydrogel earned 40 and 100.17% of their original weights (to 8.674 and 11.003 g), respectively. VD-LCP hydrogel surpasses the OD-LCP hydrogel in sorption rate as well as sorption capacity because almost all of the deliquescent salts in VD-LCP hydrogel can absorb moisture simultaneously.

Selection of the Hygroscopic Agent. Hygroscopic agents should have a good ability to sorb moisture from air and easily release water in the form of condensed water vapor at relatively low temperatures. Lithium chloride is an alternate candidate as a hygroscopic agent based on its good sorption and desorption properties. Compared with calcium chloride as a sorption agent, LiCl has the stronger ability to adsorb water from air, and it can adsorb more water than CaCl_2 under the same conditions and harvest water at very low RH under which CaCl_2 cannot work. 0.105 g LiCl can adsorb 300.95% of its weight at 50% RH and a temperature of ~ 20 °C, while 0.105 g CaCl_2 can only adsorb 199.03% of its weight under the same conditions (Figure S2). Therefore, we chose LiCl as the hygroscopic agent due to its strong ability to adsorb moisture from air, easy water-releasing, and large water capacity.

Water Sorption Property. We used the resultant LCP hydrogel to investigate its water sorption ability. In the initial stage, the hydrogel quickly sorbed moisture from the air causing a rapid increase of its weight without LiCl leakage (Figure S3). At the same time, the temperature of the hydrogel rose because deliquescent salt LiCl interacted with water molecules in the surrounding air and resulted in the release of heat energy. In addition, the experiments showed that the concentration of LiCl has a significant influence on the water sorption of LCP hydrogels, just as we expected based on the previous study.³³ Introducing LiCl within a sensible concentration range could enlarge the hygroscopicity of the hydrogel and enhance the vapor sorption ability. However, excessive amount of LiCl could diminish the solubility of polymers, decrease its swelling ratio, and reduce its water capacity. When LiCl concentration increases to 0.8 g g^{-1} , it diminishes the swelling ratio of CNT-PAm to zero.^{34,35} Therefore, we set the LiCl concentration range from 0.2 to 0.5 g g^{-1} . As shown in Figure 3a,b, LCP hydrogels with LiCl concentrations of 0.3 and 0.4 g g^{-1} give the best two

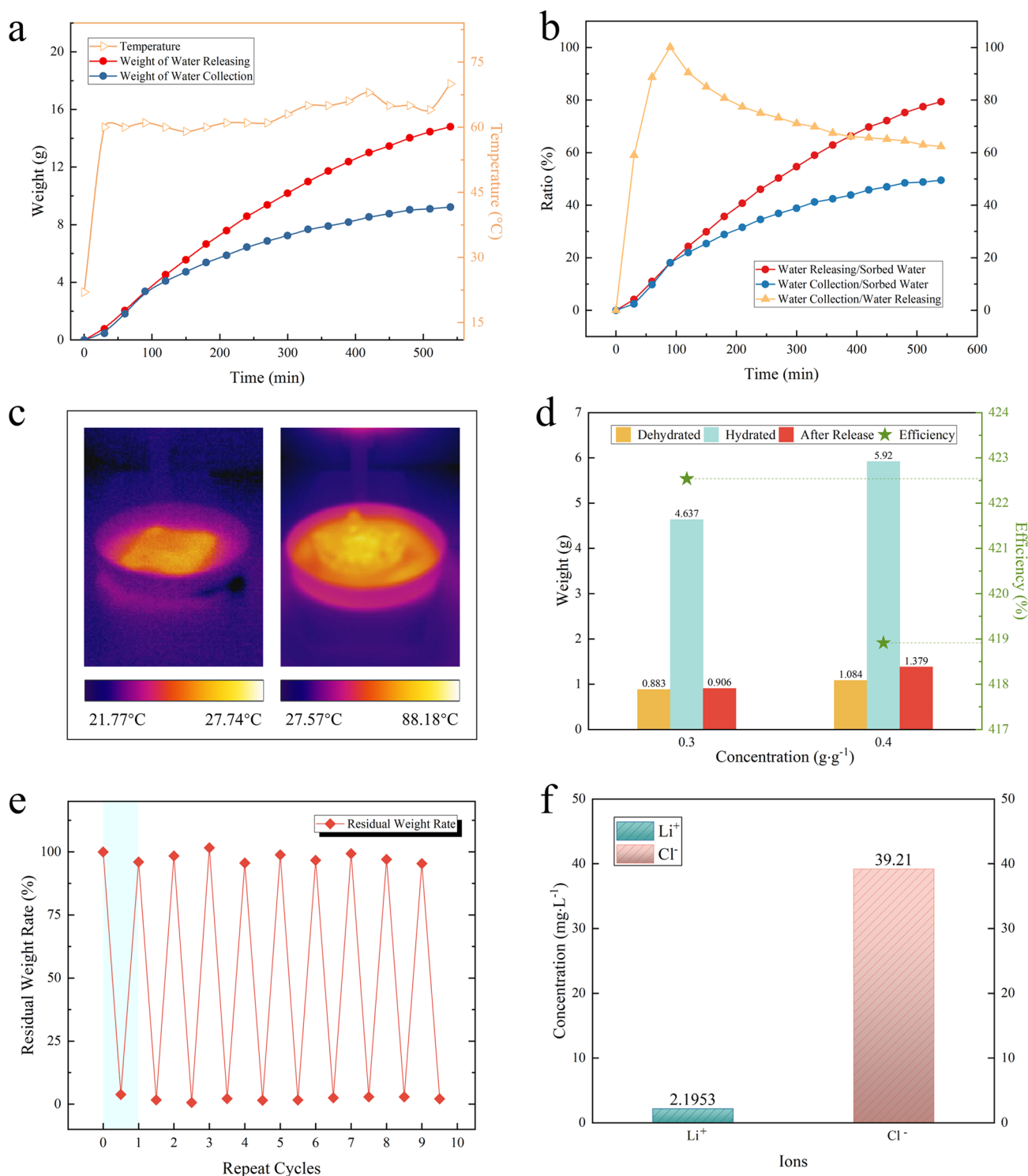


Figure 4. Water desorption properties. (a) Temperature and weight of water releasing and water collection during the release process. (b) Ratio of water releasing to sorbed water, water collection to sorbed water, and water collection to water releasing. (c) Thermal images of LCP hydrogel in the beginning and after 3 h when releasing water with the increase of temperature. (d) Weight of LCP hydrogel with LiCl concentrations of 0.3 and 0.4 g g⁻¹ in dehydrated, hydrated, and after-releasing state, and their efficiencies. (e) 10-cycled durability test of LCP hydrogel for AWH. Blue shade indicates the first full cycle of sorption release. Sorption happened under a RH of 98% for 19 h. Desorption was conducted under an ultraviolet blended mercury lamp with a light intensity of 500 W m⁻² for 5 h. Residual weight rate was calculated as: weight increment divided by water load at the beginning of the first cycle. (f) Ionic concentration of the collected water.

performances of capturing water, gaining 77.56 and 95.73% of their original weights (4.903 to 8.706 g and 5.802 to 11.356 g within 330 min at 60% RH, temperature of 16–20 °C, respectively) compared with LCP hydrogels with LiCl

concentrations of 0.2 and 0.5 g g⁻¹, which gained 66.18 and 49.75% of their original weights (3.847 to 6.393 g and 6.398 to 9.581 g within 330 min at 60% RH, temperature of 16–20 °C, respectively). In other time periods with RH between 80 and

90%, a similar trend of water capturing of LCP hydrogels with different LiCl concentrations can also be observed. As shown in Figure 3c,d, LCP hydrogels with LiCl concentrations of 0.3 and 0.4 g g⁻¹ also demonstrated the best two water-capturing abilities at 80–90% RH and gained 119.13 and 145.40% of their original weights (4.573 to 12.409 g and 5.915 to 13.318 g within 330 min at 80–90% RH, temperature of 14–18 °C, respectively). On the other hand, LCP hydrogels with LiCl concentrations of 0.2 and 0.5 g g⁻¹ only sorbed 111.81 and 115.97% of their original weights (3.376 to 8.023 g and 6.812 to 14.712 g within 330 min at 80–90% RH, temperature of 14–18 °C, respectively). This result proves again that LCP hydrogels with 0.4 and 0.3 g g⁻¹ LiCl have the largest and the second large water capacities. The sorption experiments of LCP hydrogel with 0.3 and 0.4 g g⁻¹ LiCl, performed in a 25 °C humidity chamber, resulted in gaining 79 and 97% of their own weights at 30% RH (0.56 to 1.00 g and 0.70 to 1.38 g), 102 and 120% of their own weights at 60% RH (0.84 to 1.70 g and 0.64 to 1.41 g), 144 and 184% of their own weights at 90% RH (0.98 to 2.39 g and 0.87 to 2.47 g) within 10 h, respectively (Figure 3e–g). As for the performance within 24 h at the same temperature of 25 °C, the water sorption rates of LCP hydrogels with 0.3 and 0.4 g g⁻¹ LiCl were 91.37 and 124.21% of their own weights under 30% RH (0.56 to 1.07 g and 0.7 to 1.57 g), 132.14 and 154.69% of their own weights under 60% RH (0.84 to 1.95 g and 0.64 to 1.63 g), and 176.53 and 217.24% of their own weights under 90% RH (0.98 to 2.71 g and 0.87 to 2.76 g), respectively. Likewise, the performance of LCP hydrogel with 0.4 g g⁻¹ LiCl is still the best. Compared with the water capacity of the LCP hydrogel with 0.3 g g⁻¹ LiCl at 30, 60, and 90% RH (91.37, 132.14, and 176.53% of their own weights), water sorbed by LCP hydrogels with 0.4 g g⁻¹ LiCl at 30, 60, and 90% RH (124.21, 154.69, and 217.24% of their own weights) are 32.84, 22.55, and 40.71% higher (Figure 3h).

In addition, the LCP hydrogel can achieve AWH with a broad range of sorption RH from 100% to even lower than 20%, which makes it possible to collect water in some extreme conditions. LCP hydrogel can rapidly capture water vapor from the atmosphere, which differs from other bulk-like hydrogels used in AWH previously reported (Table S2). Moreover, the sorption efficiency is as high as 0.32 g g⁻¹ h⁻¹ in the first 3 h at 90% RH and temperature of 25 °C. Compared with some other hydrogels, LCP hydrogel also shows a unique water-uptake ability (Table S3), and the highest water-sorption capacity of LCP hydrogel can reach up to 433.72% of its own weight at 98% RH and temperature of 25 °C within 60 h.

Water Release Property. To investigate water release properties, we put a 26.952 g hydrogel (8.306 g of dry weight) into a homemade water-release device. Due to the great thermal stability of LCP hydrogel (Figure S4), we desorbed the captured water in the LCP hydrogel via the photothermal effect. In the first stage, the temperature of the hydrogel drastically decreased from room temperature to 60 °C within 30 min and stayed 60–70 °C during the whole desorption process in the container under 300 W m⁻² light. Finally, the weight of the LCP hydrogel decreased down to 12.147 g at the end of a 9 h desorption. The LCP hydrogel lost 14.795 g of weight, namely, 79.35% of the captured water. The device collected 9.227 g of the water, which is 49.49% of the captured water and 62.37% of the released water (Figure 4a,b). In another desorption test without a container under 500 W m⁻² light, the temperature of the LCP hydrogel gradually rose and reached 82.71 °C within 3 h (Figure 4c). We also found that the collected water had started being released

when the temperature of the LCP hydrogel reached ~50 °C, and the high temperatures were more conducive to water release, showing that LCP hydrogel has a great water-release ability. This is because the homogeneously scattered CNTs in the LCP hydrogel not only helped transport the water into the hydrogel but also absorbed light and transferred light into thermal energy. Moreover, the UV–vis–NIR absorption spectra between 250 and 2500 nm were provided to prove that CNT-COOHs helped increase the light absorption of the hydrogel (Figure S5).

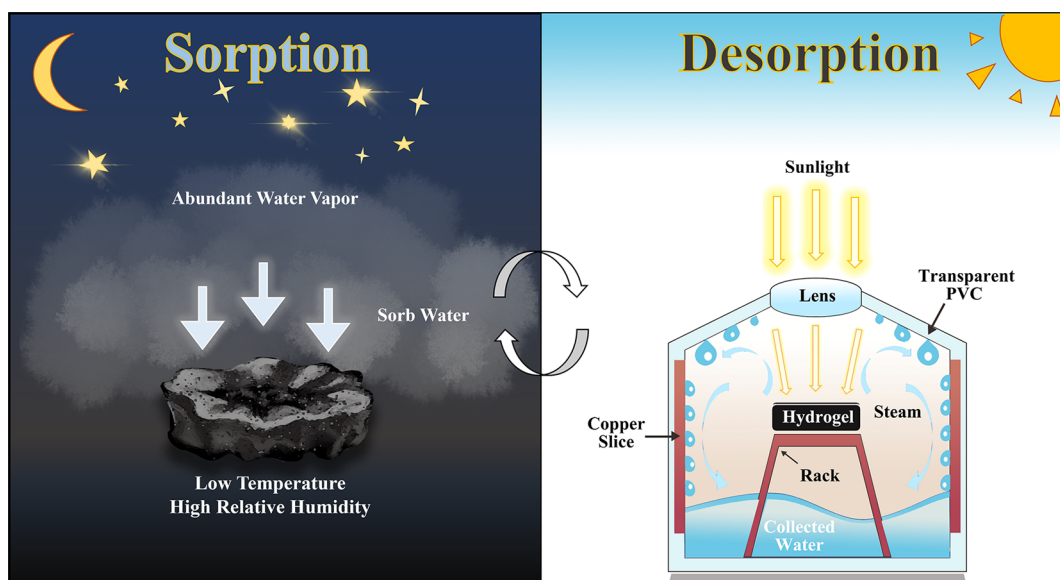
Furthermore, we conducted a sorption–desorption test to show, which LiCl concentration endows the LCP hydrogel with best harvesting efficiency without a container under 500 W m⁻² light. The result showed that 0.883 g LCP hydrogel with 0.3 g g⁻¹ LiCl lost 3.731 g of water, which was 99.38% of the collected water and 422.54% of its original weight, while 1.084 g LCP hydrogel with 0.4 g g⁻¹ LiCl lost 4.541 g of water, which was 93.89% of the collected water and 418.91% of its original weight, as shown in Figure 4d. Although LCP hydrogel with a LiCl concentration of 0.4 g g⁻¹ sorbs more water than LCP hydrogel with a LiCl concentration of 0.3 g g⁻¹, the latter one has a better harvesting efficiency (422.54%). Therefore, we decided 0.3 g g⁻¹ to be the proper LiCl concentration for AWH.

Meanwhile, we also investigated the water sorption of LCP hydrogel with 0.3 g g⁻¹ LiCl in an outdoor environment. The results showed that the LCP hydrogel with 0.3 g g⁻¹ LiCl can collect 4.151, 5.745, and 6.524 g of water (5.176 to 9.327 g, 5.103 to 10.848 g, and 4.207 to 10.731 g, corresponding to 80.20, 112.58, and 155.08% of their own weights) within 7 h at 60–70% RH, 80% RH, and 90% RH (Figure S6), respectively, demonstrating great outdoor water-sorption ability of the LCP hydrogel.

Durability of the LCP Hydrogel. We conducted a durability test with 10 full cycles of sorption–desorption using an LCP hydrogel (dry weight 2.382 g) with 0.3 g g⁻¹ LiCl. At the beginning of the first cycle, hydrogel already carried 6.403 g of water. As shown in Figure 4e, the LCP hydrogel demonstrates a similar residual weight rate during each cycle. Similar water yields were also presented in every cycle during the durability test, enabling long-term water harvesting. During this test, sorption rate and desorption rate fluctuated in an acceptable range due to the environmental influence. There is no obvious decline in sorption capacity and desorption capacity. Therefore, the long-term durability of our LCP hydrogel enables repeated water collection over time.

Water Quality Assessment. The released water was gathered for the ionic concentration test. The result shows the lithium-ion concentration is 2.195 mg L⁻¹ and chloride's concentration is 39.210 mg L⁻¹ (Figure 4f). The WHO guideline value for drinking water salinity is 250 mg of chloride per liter for chloride;³⁶ thus, it is within the safe range. Namely, the water produced by the LCP hydrogel is qualified as potable water.

AWH of the LCP Hydrogel. We presented a macroporous hydrogel with a high water uptake and rigid sorption rate. As a solid sorbent, it is easy to be set in the handmade device (Figure S7). Although sorption can happen at any time of the day, it was still planned to sorb water vapor at night with abundant atmospheric water vapor and low ambient temperature, which are in favor of increment of water uptake. Water release was realized by placing the device under natural sunlight. Normally, substance with the intrinsic traits of high thermal radiation and thermal conductivity is the most suitable material for decorating the device. Droplets are easily formed on the walls of the device

Scheme 2. Schematic Diagram of LCP Hydrogel for Atmospheric Water Harvesting^a

^aThe diagram illustrates the two processes of LCP hydrogel during water harvesting. First, LCP hydrogel sorbs moisture from air at night when temperature is relatively low, and RH is relatively high. Later, desorption happens in a homemade device when heated by sunlight. As the temperature climbs, water in the hydrogel starts to evaporate. Water vapor condenses into liquid water which was then collected in the homemade device.

while the water yield increases, as a result of radiational cooling (Scheme 2). On the campus of the Northeastern University of China, mean RH can reach up to 90% on summer nights. In accordance with the outdoor sorption test, the LCP hydrogel with 0.3 g g^{-1} LiCl can sorb 97.95% its weight within 3 h under 90% RH, $25 \text{ }^\circ\text{C}$ (0.98 to 1.94 g). Additionally, LCP hydrogel with 0.3 g g^{-1} LiCl can release 1.23 g g^{-1} water and collect 0.87 g g^{-1} water within 5 h with a light intensity of 300 W m^{-2} (Figure S8). We arranged a 3 h sorption, followed by a 5 h desorption, and the whole process can cycle three times a day, which means 1 kg of LCP hydrogel can create 2.56 L of water within a day at 90% RH, $25 \text{ }^\circ\text{C}$. Therefore, it is estimated that the daily water yield can reach up to approximately $2.56 \text{ kg kg}^{-1} \text{ day}^{-1}$ at 90% RH, $25 \text{ }^\circ\text{C}$, enabling daily water consumption of an adult.

CONCLUSIONS

In conclusion, we employed an innovative strategy of PFVD to rationally fabricate macroporous polymeric hydrogel in a simple and low-cost manner for high-performance AWH. The macroporous hydrogel with a high specific surface area enables sufficient contact of inner sorbent and outside humid air. The macroporous hydrogel demonstrates high-performance AWH with a broad range of sorption humidity (RH from 100% to even lower than 20%), high water sorption capacity (highest $\sim 433.72\%$ of hydrogel's own weight), rapid vapor capturing (the sorption efficiency is as high as $0.32 \text{ g g}^{-1} \text{ h}^{-1}$ in the first 3 h), unique durability, low desorption temperature ($\sim 50 \text{ }^\circ\text{C}$, lowest), and high water-releasing rate (up to $\sim 99.38\%$). The experiments demonstrate that the LCP hydrogel with a LiCl concentration of 0.3 g g^{-1} had the best water harvesting efficiency. When fully exposed to the humid environment, LCP hydrogel has a maximum water load capacity of $\sim 4.34 \text{ g g}^{-1}$ and releases as high as $\sim 99.38\%$ of the collected water via the photothermal effect under 500 W m^{-2} light. In addition, it is estimated that the daily water yield can reach up to approximately $2.56 \text{ kg kg}^{-1} \text{ day}^{-1}$. The LCP hydrogel shows

great potential for AWH under many types of weather, even for terribly low humid conditions, and being deployed in distressed and remote areas. Our high-performance, affordable, and easy-to-scale-up LCP hydrogel can not only create opportunities for large-scale and high-performance AWH but also offer potential candidates for functional material, soft matter, flexible electronics, sensor, wearable device, tissue engineering, and biomedical applications.

EXPERIMENTAL SECTION

Fabrication of the LCP Hydrogel. Acrylamide (AM, 99%, Aladdin), potassium persulfate (KPS, 99.99%, Aladdin), *N,N'*-methylenebis(acrylamide) (MBAA, 99%, Aladdin), *N,N,N',N'*-tetramethylethylenediamine (TEMED, 99%, Aladdin), lithium chloride (LiCl, 99%, Aladdin), calcium chloride (CaCl_2 , 96%, Aladdin), polyethylene glycol with a molecular weight of 400 (PEG-400, Aladdin), carboxylic multi-walled carbon nanotubes (CNT-COOHs, $5^{-1} 5 \text{ nm} \times 0.5\text{--}2 \text{ }\mu\text{m}$, XFNANO), and polyethyleneglycol-mono-[*p*-(1,1,3,3-tetramethylbutyl)-phenyl]-ether, Octoxynol 9 (Triton X-100, 99.5%, BioFroxx) were used without further purification. Deionized (DI) water ($18.2 \text{ M}\Omega$, from UPTA-UV-20) was used during the whole process.

First, we prepared a precursor solution. We dissolved 3 mg CNT-COOHs into 10 mL water by sonification and then added 2 g AM into the CNT-COOH-dispersion solution. We used nitrogen to remove the oxygen in the solution. After deoxidization, we put 3 mg MBAA as the cross-linking agent and then 6 mg APS as the initiator into the dispersion solution. Later, 2.2 mL PEG-400 as the pore-forming agent was introduced into the solution. Finally, the precursor solution was prepared successfully. Next, 100 μL TEMED as the accelerator was added into the precursor solution. Then, the hydrogel can be obtained after 12 h at room temperature. Subsequently, we immersed the hydrogel in excess DI water for 24 h to remove the remaining monomer. After freeze-drying, the hydrogel was soaked in a LiCl solution with fixed concentrations for 24 h. At last, LCP hydrogel was obtained after second-time freeze-drying.

Instruments and Characterization. The thermal stability of LCP hydrogel was measured with a thermo gravimetric analysis (TGA) (TGA/DSC3+, METTLER TOLEDO, Switzerland). The component

of LCP hydrogel was manifested in a FTIR transmittance spectrum (VERTEX70, Bruker, German). UV–vis–NIR spectrum was measured by a UV–vis–NIR spectrophotometer (UH4150, HITACHI, Japan). The surface morphology was investigated using a scanning electron microscope (EVO 18, Carl Zeiss, German with EHT 20 kV and MAG 50,250, and 500X). Infrared image was captured by a thermal imager (HM-TPH11-3AXF, HIKVISION, China). The temperature of the hydrogel was measured by a thermal couple (UT320A, UNI-T, China). The velocity of air flow was measured by an air-flow anemometer (AS806, SMART SENSOR, China). Light intensity was measured by a solar power meter (SM206-SOLAR, SANPOMETER, China). Samples were freeze-dried by a freeze dryer (FD-A12N-80, KUANSONS, China). Indoor sorption experiments were conducted in a humidity chamber (HMS-30B, MS SHIMEI, China). An ultraviolet blended mercury lamp (SPARKZOO, 65W, CHANGZHOU SPARK LIGHTING CO., LTD, China) was used during release experiments. Concentration of chloride in collected water was tested by a high-pressure ion chromatography (DIONEX-ICS-6000, Thermo Fisher Scientific, America). Concentration of lithium in collected water was tested by an inductively coupled plasma optical emission spectrometer (ICP-OES 730, Agilent, America).

Sorption Experiments. Sorption tests of OD LCP hydrogel and VD LCP hydrogel were conducted in natural surroundings. After the drying process, LCP hydrogels with a LiCl concentration of 0.3 g g⁻¹ were placed outside the building. We measured their weights every 30 min. We operated the experiment at 60–70% RH and 80–90% RH, ~20 °C, air flow both between 0.5 and 2 m s⁻¹ separately to roundly measure subjects.

The test of sorption ability of deliquescent salts happened in a closed room with temperatures varied between 23 and 25 °C, no observable air flow, and RH fluctuated between 47 and 50%. The same amount of anhydrous LiCl and CaCl₂ were tiled on a flat plate for 3 days.

To find out which LiCl concentration enlarges the water sorption capacity of CNT-PAM hydrogel varied from 0.2 to 0.5 g g⁻¹, we conducted several experiments both outdoor and indoor. Outdoor sorption experiments were carried out under different weather conditions on the campus of the Northeastern University in Shenyang, China. On a rainy night, the RH was around 80–90%, the temperature was between 14 and 19 °C, and air velocity was 0.3–1.2 m s⁻¹. RH at night without rain was down to 60–70%, the temperature was 18–24 °C, and air velocity was 0.8–1.7 m s⁻¹ (outdoor temperatures varied on account of different weathers). We kept tracking their weights and RH every 30 min for 330 min. Indoor sorption experiments of LCP hydrogels with LiCl concentrations of 0.3 and 0.4 g g⁻¹ were conducted in a humidity chamber at 30, 60, and 90% RH with an air velocity of 0.78 m s⁻¹ to test its sorption capacity thoroughly. The weights of hydrogels were recorded every hour for 10 h, but the sorption did not stop after another 14 h, and the results were noted.

Desorption Experiments. A hydrated LCP hydrogel was placed into a device composed of a transparent shell, a convex lens, and metal foil. A convex lens set on top of the shell is for concentrating sunlight. Metal foil stuck to the walls of the shell was for temperature cooling. The LCP hydrogel along with the device was put under an ultraviolet blended mercury lamp with a light intensity of ~300 W m⁻² for 540 min. The weights of LCP hydrogel and collected water in the device were measured every 30 min. The LCP hydrogel was directly exposed under an ultraviolet blended mercury lamp with a light intensity of ~500 W m⁻² to capture its IR image, track its temperature by a thermal couple, and record its weight change.

The durability test was completed by repeating the water-harvesting circle 10 times, which comprised a 19 h sorption at 98% RH in a humidity chamber and a 5 h desorption under an ultraviolet-blended mercury lamp with a light intensity of 500 W m⁻². The weight of LCP hydrogel was measured after every process.

LCP hydrogels with LiCl concentrations of 0.3 and 0.4 g g⁻¹ were loaded with water after 48 h sorption in a humidity chamber at a RH of 98%. A 6 h desorption procedure under the ultraviolet blended mercury lamp with a light intensity of 500 W m⁻² was arranged tandemly. This aims to compare the water harvesting efficiency of LCP hydrogels with different LiCl concentrations.

Furthermore, we put an LCP hydrogel on a hollowed plastic basket with a copper slice under the shelf and set the device in a room with a RH of 50–60% and temperature around 20 °C for 14 days to see if there is any LiCl leakage.

The outdoor sorption tests of LCP hydrogels with 0.3 g g⁻¹ LiCl were conducted for three nights with different environmental conditions. RH was 60–70% on the first night, and temperature was 23–26 °C with an air velocity of 0.1–0.7 m s⁻¹. RH was around 80% on the second night, and temperature was 19–22 °C with an air velocity of 0.1–0.5 m s⁻¹. RH was about 90% on the last night, and temperature was 23–26 °C with an air velocity of 0.1–0.9 m s⁻¹ (outdoor temperatures varied on account of different weathers).

CALCULATION

Weight change rate was calculated as

$$\text{weight change rate} = \frac{\Delta m}{m_o} \times 100\% \quad (1)$$

$$\Delta m = m_{\text{current}} - m_o \quad (2)$$

Residual weight rate in the durability test was calculated as follows

$$\text{residual weight rate} = \frac{\Delta m}{m_{\text{sorbed}}} \times 100\% \quad (3)$$

Harvesting efficiency was calculated as follows

$$\text{harvesting efficiency} = \frac{m_{\text{released}}}{m_o} \times 100\% \quad (4)$$

In addition, m_{current} , m_o , and m_{released} represent the current weight, original dry weight of the hydrogel, and weight of water released from hydrogels. In the calculation of residual weight rate, m_{sorbed} stands for the weight of water originally carried by the hydrogel at the beginning of the test.

ASSOCIATED CONTENT

Supporting Information

The Supporting Information is available free of charge at <https://pubs.acs.org/doi/10.1021/acsami.2c04228>.

Cost calculation, sorption rate comparison, maximum water uptake comparison, FTIR results, weights of CaCl₂ and LiCl, digital image of corrosion experiment, TGA result, UV–vis–NIR results, weight change rate of the LCP hydrogel, digital image of the photothermal evaporation device, and water release and water collection of the LCP hydrogel (PDF)

Hydrophilicity of VD and OD hydrogel (MP4)

AUTHOR INFORMATION

Corresponding Author

Ye Tian – College of Medicine and Biological Information Engineering, Northeastern University, Shenyang 110169, China; Foshan Graduate School of Northeastern University, Foshan 528300, China; orcid.org/0000-0003-2134-1536; Email: tianye@bmie.neu.edu.cn

Authors

Tong Lyu – College of Medicine and Biological Information Engineering, Northeastern University, Shenyang 110169, China; orcid.org/0000-0002-1487-5970

Zhaoyang Wang – College of Medicine and Biological Information Engineering, Northeastern University, Shenyang 110169, China

Ruonan Liu – College of Medicine and Biological Information Engineering, Northeastern University, Shenyang 110169, China

Kun Chen – College of Medicine and Biological Information Engineering, Northeastern University, Shenyang 110169, China; orcid.org/0000-0002-1991-6217

He Liu – College of Medicine and Biological Information Engineering, Northeastern University, Shenyang 110169, China

Complete contact information is available at:
<https://pubs.acs.org/10.1021/acsami.2c04228>

Author Contributions

T.L. and Y.T. designed the project. T.L. performed the experiments. T.L., Z.W., and R.L. analyzed the experimental data. T.L., K.C., and H.L. drew the figures. T.L. and Y.T. wrote the manuscript. Y.T. supervised the study. All authors commented on the paper.

Notes

The authors declare no competing financial interest.

ACKNOWLEDGMENTS

Financial support from Guangdong Basic and Applied Basic Research Foundation (2020A1515110126 and 2021A1515010130) and the Fundamental Research Funds for the Central Universities (N2119006 and N2224001-10) is gratefully acknowledged.

REFERENCES

- (1) Liu, J.; Yang, H.; Gosling, S. N.; Kumm, M.; Flörke, M.; Pfister, S.; Hanasaki, N.; Wada, Y.; Zhang, X.; Zheng, C.; Alcamo, J.; Oki, T. Water Scarcity Assessments in the Past, Present and Future. *Earth's Future* **2017**, *5*, 545–559.
- (2) Li, R.; Shi, Y.; Alsaedi, M.; Wu, M.; Shi, L.; Wang, P. Hybrid Hydrogel with High Water Vapor Harvesting Capacity for Deployable Solar-Driven Atmospheric Water Generator. *Environ. Sci. Technol.* **2018**, *52*, 11367–11377.
- (3) Seo, D.; Lee, C.; Nam, Y. Influence of Geometric Patterns of Microstructured Superhydrophobic Surfaces on Water-harvesting Performance via Dewing. *Langmuir* **2014**, *30*, 15468–15476.
- (4) Gandhidasan, P.; Abualhamayel, H. I. Modeling and Testing of a Dew Collection System. *Desalination* **2005**, *180*, 47–51.
- (5) Lee, A.; Moon, M.-W.; Lim, H.; Kim, W.-D.; Kim, H.-Y. Water Harvest via Dewing. *Langmuir* **2012**, *28*, 10183–10191.
- (6) LaPotin, A.; Kim, H.; Rao, S. R.; Wang, E. N. Adsorption-Based Atmospheric Water Harvesting: Impact of Material and Component Properties on System-Level Performance. *Acc. Chem. Res.* **2019**, *52*, 1588–1597.
- (7) Zhang, F.; Guo, Z. Bioinspired Materials for Water-harvesting: Focusing on Microstructure Designs and the Improvement of Sustainability. *Mater. Adv.* **2020**, *1*, 2592–2613.
- (8) Zhang, S.; Huang, J.; Chen, Z.; Lai, Y. Bioinspired Special Wettability Surfaces: From Fundamental Research to Water Harvesting Applications. *Small* **2017**, *13*, 1602992–1603020.
- (9) Tian, Y.; Zhu, P.; Tang, X.; Zhou, C.; Wang, J.; Kong, T.; Xu, M.; Wang, L. Large-scale Water Collection of Bioinspired Cavity-microfibers. *Nat. Commun.* **2017**, *8*, 1080.
- (10) Venkatesan, H.; Chen, J.; Liu, H.; Liu, W.; Hu, J. A Spider-Capture-Silk-Like Fiber with Extremely High-Volume Directional Water Collection. *Adv. Funct. Mater.* **2020**, *30*, 2002437–2002445.
- (11) Wang, X.; Zeng, J.; Li, J.; Yu, X.; Wang, Z.; Zhang, Y. Beetle and Cactus-inspired Surface Endows Continuous and Directional Droplet Jumping for Efficient Water Harvesting. *J. Mater. Chem. A* **2021**, *9*, 1507–1516.
- (12) Bai, H.; Zhao, T.; Wang, X.; Wu, Y.; Li, K.; Yu, C.; Jiang, L.; Cao, M. Cactus Kirigami for Efficient Fog Harvesting: Simplifying a 3D Cactus into 2D Paper Art. *J. Mater. Chem. A* **2020**, *8*, 13452–13458.
- (13) Yu, Z.; Yun, F. F.; Wang, Y.; Yao, L.; Dou, S.; Liu, K.; Jiang, L.; Wang, X. Desert Beetle-Inspired Superwetttable Patterned Surfaces for Water Harvesting. *Small* **2017**, *13*, 1701403–1701409.
- (14) White, B.; Sarkar, A.; Kietzig, A.-M. Fog-harvesting Inspired by the Stenocara Beetle—an Analysis of Drop Collection and Removal from Biomimetic Samples with Wetting Contrast. *Appl. Surf. Sci.* **2013**, *284*, 826–836.
- (15) Dai, X.; Sun, N.; Nielsen, S. O.; Stogin, B. B.; Wang, J.; Yang, S.; Wong, T.-S. Hydrophilic Directional Slippery Rough Surfaces for Water Harvesting. *Sci. Adv.* **2018**, *4*, No. eaq0919.
- (16) Gao, F.; Yao, Y.; Wang, W.; Wang, X.; Li, L.; Zhuang, Q.; Lin, S. Light-Driven Transformation of Bio-Inspired Superhydrophobic Structure via Reconfigurable PAzoMA Microarrays: From Lotus Leaf to Rice Leaf. *Macromolecules* **2018**, *51*, 2742–2749.
- (17) Wang, Y.; Liang, X.; Ma, K.; Zhang, H.; Wang, X.; Xin, J. H.; Zhang, Q.; Zhu, S. Nature-Inspired Windmill for Water Collection in Complex Windy Environments. *ACS Appl. Mater. Interfaces* **2019**, *11*, 17952–17959.
- (18) Kurt, S.; Harry, W. G. Water Collection and Drinking in Phrynocephalus Helioscopus A Possible Condensation Mechanism. *J. Herpetol.* **1987**, *21*, 134–139.
- (19) Asim, N.; Badiei, M.; Alghoul, M. A.; Mohammad, M.; Samsudin, N. A.; Amin, N.; Sopian, K. Sorbent-based Air Water-harvesting Systems: Progress, Limitation, and Consideration. *Rev. Environ. Sci. Bio.* **2020**, *20*, 257–279.
- (20) Kumar, M.; Yadav, A. Composite Desiccant Material “CaCl₂/Vermiculite/Saw wood”: a New Material for Fresh Water Production from Atmospheric Air. *Appl. Water Sci.* **2016**, *7*, 2103–2111.
- (21) William, G. E.; Mohamed, M. H.; Fatouh, M. Desiccant System for Water Production from Humid Air Using Solar Energy. *Energy* **2015**, *90*, 1707–1720.
- (22) Srivastava, S.; Yadav, A. Extraction of Water Particles from Atmospheric Air through a Scheffler Reflector Using Different Solid Desiccants. *Int. J. Ambient Energy* **2018**, *41*, 1357–1369.
- (23) Kumar, M.; Yadav, A. Solar-driven Technology for Freshwater Production from Atmospheric Air by Using the Composite Desiccant Material “CaCl₂/Floral Foam”. *Environ. Dev. Sustain.* **2015**, *18*, 1151–1165.
- (24) Kalmutzki, M. J.; Diercks, C. S.; Yaghi, O. M. Metal-Organic Frameworks for Water Harvesting from Air. *Adv. Mater. Interfac.* **2018**, *30*, 1704304–1704329.
- (25) Hanikel, N.; Prévot, M. S.; Yaghi, O. M. MOF Water Harvesters. *Nat. Nanotechnol.* **2020**, *15*, 348–355.
- (26) Maher, H.; Rupam, T. H.; Rocky, K. A.; Bassiouny, R.; Saha, B. B. Silica Gel-MIL 100(Fe) Composite Adsorbents for Ultra-low Heat-driven Atmospheric Water Harvester. *Energy* **2022**, *238*, 121741–121750.
- (27) Srivastava, S.; Yadav, A. Water Generation from Atmospheric Air by Using Composite Desiccant Material through Fixed Focus Concentrating Solar Thermal Power. *Sol. Energy* **2018**, *169*, 302–315.
- (28) Jia, C. X.; Dai, Y. J.; Wu, J. Y.; Wang, R. Z. Experimental Comparison of Two Honeycombed Desiccant Wheels Fabricated with Silica Gel and Composite Desiccant Material. *Energy Convers. Manag.* **2006**, *47*, 2523–2534.
- (29) Zhou, X.; Lu, H.; Zhao, F.; Yu, G. Atmospheric Water Harvesting: A Review of Material and Structural Designs. *ACS Mater. Lett.* **2020**, *2*, 671–684.
- (30) Rosinger, A. Y.; Herrick, K. A.; Wutich, A. Y.; Yoder, J. S.; Ogdan, C. L. Disparities in Plain, Tap and Bottled Water Consumption among US Adults: National Health and Nutrition Examination Survey (NHANES) 2007-2014. *Public Health Nutr.* **2018**, *21*, 1455–1464.
- (31) Meinder, A.-J.; Meinders, A. E. Hoeveel Water Moeten We Eigenlijk Drinken? [How Much Water Should We Actually Drink?]. *Ned. Tijdschr. Geneesk.* **2010**, *154*, A1757.

(32) Zhang, X.-Z.; Yang, Y.-Y.; Chung, T.-S.; Ma, K.-X. Preparation and Characterization of Fast Response Macroporous Poly(N-isopropylacrylamide) Hydrogels. *Langmuir* **2001**, *17*, 6094–6099.

(33) Ahmed, S. Y.; Gandhidasan, P.; Al-Farayedhi, A. A. Thermodynamic Analysis of Liquid Desiccants. *Sol. Energy* **1998**, *62*, 11–18.

(34) Kang, B.; Tang, H.; Zhao, Z.; Song, S. Hofmeister Series: Insights of Ion Specificity from Amphiphilic Assembly and Interface Property. *ACS Omega* **2020**, *5*, 6229–6239.

(35) Aleid, S.; Wu, M.; Li, R.; Wang, W.; Zhang, C.; Zhang, L.; Wang, P. Salting-in Effect of Zwitterionic Polymer Hydrogel Facilitates Atmospheric Water Harvesting. *ACS Mater. Lett.* **2022**, *4*, 511–520.

(36) WHO *Guidelines for Drinking-Water Quality. Guidelines for Drinking-Water Quality*, 2003; pp 324–325.

Recommended by ACS

Sustainable Self-Cleaning Evaporators for Highly Efficient Solar Desalination Using a Highly Elastic Sponge-like Hydrogel

Aqiang Chu, Hao Li, *et al.*

AUGUST 01, 2022

ACS APPLIED MATERIALS & INTERFACES

READ 

Highly Efficient Solar Evaporator Based On a Hydrophobic Association Hydrogel

Xiaoyu Zhang, Rong Ran, *et al.*

DECEMBER 02, 2020

ACS SUSTAINABLE CHEMISTRY & ENGINEERING

READ 

Composite Polyelectrolyte Photothermal Hydrogel with Anti-biofouling and Antibacterial Properties for the Real-World Application of Solar Steam Generation

Bolun Peng, Peng Wang, *et al.*

APRIL 01, 2022

ACS APPLIED MATERIALS & INTERFACES

READ 

Surface Patterning of Two-Dimensional Nanostructure-Embedded Photothermal Hydrogels for High-Yield Solar Steam Generation

Yi Lu, Xiaofei Yang, *et al.*

JUNE 10, 2021

ACS NANO

READ 

Get More Suggestions >